# Robust 3D Distributed Formation Control with Collision Avoidance and Application to Multirotor Aerial Vehicles

Kaveh Fathian, Sleiman Safaoui, Tyler H. Summers, Nicholas R. Gans.

***Abstract*— We present a distributed control strategy for a team of agents to autonomously achieve a desired 3D formation. Our approach is based on local relative position measurements and can be applied to multirotor aerial vehicles. We assume that agents have a common sense of direction, which is used to align the $z$-axes of their local coordinate frames. However, this assumption is not crucial, and our approach is provably robust to misalignments in the local coordinate frames or measurement inaccuracies. In particular, agents can move along any direction that projects positively onto the desired direction of motion. This property is exploited to design a fully-distributed collision avoidance strategy. We validate the proposed approach experimentally and show that a team of quadrotors can achieve a desired 3D formation without collisions.**

***Index Terms*— Multi-robot systems, distributed robotic systems, 3D formation control, distributed collision avoidance.**

## Supplementary Material

Video of the paper summary and experiments is available at https://youtu.be/sCPT4QVLD8A. Code and experimental setup details are accessible at https://goo.gl/PN5L5Z.

## I. Introduction

A team of unmanned aerial vehicles can be used to collaboratively map and monitor an unknown environment [1], inspect infrastructures [2], deliver goods [3], or manipulate objects [4]. In these applications, the ability to bring the vehicles to a desired geometric shape (i.e., formation) is a fundamental building block upon which more sophisticated maneuvering and navigation policies can be constructed.

There exists a large body of work on formation control of autonomous vehicles [5]–[7]. However, many methods rely on a centralized motion planning scheme or a global positioning/communication paradigm [8]–[11]. Fully distributed formation control strategies [12]–[15], on the other hand, do not have these requirements and in comparison have better scalability, naturally parallelized computation, and resiliency to global positioning signal jamming or loss.

In this work, we present a distributed control strategy for a team of distinct agents to achieve a desired 3D formation. We assume that agents have a common sense of direction, which is used to align the $z$-axes of their local coordinate frames. Our approach can be applied to multirotor aerial vehicles (MAVs), where the direction of gravitational force, measured by an onboard IMU sensor, can be used to align the local $z$-axes. Furthermore, visual sensors can be used to estimate the relative positions of the neighboring MAVs [16]. In our approach, a set of constant gain matrices computed by solving a semidefinite program (SDP) is provided to each agent before the mission. The local relative positions of neighboring agents are multiplied by the associate gain matrices and summed to derive a desired direction of motion throughout the mission. When necessary, a distributed collision avoidance algorithm changes the desired direction to prevent agents from getting closer than a desired distance.

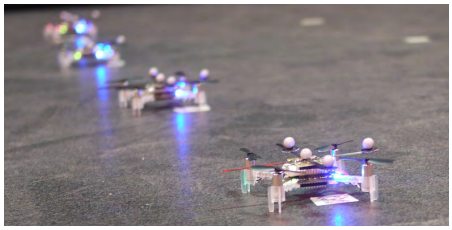

Fig. 1. Crazyflie quadrotors used to achieve a 3D formation.

The main contributions of this paper include an extension of our previous work on planar formations [17], [18] to 3D formations, the addition of a collision avoidance strategy, and experimental validations (Fig. 1). In particular, we extend our SDP gain design approach to 3D shapes and prove that convergence to the desired formation is guaranteed when agents move along any arbitrary direction that projects positively onto the desired direction of motion determined by the control strategy. Our approach does not require global position information (such as GPS measurements), can be applied on existing MAV platforms, and is provably robust to noise, disturbances, and forces that may affect the estimated direction of gravity[1].

Existing literature closely related to this work include [15], [20]–[22]. The approach presented in [21] is based on *affine* 3D formations, which are not rigid geometrically. To make the shape rigid, a leader-follower scheme is considered in [15]. In comparison, in our proposed strategy, all agents actively participate in controlling the formation shape. The control in [20] is based on a common $z$-direction, which is also the assumption of this paper. Compared to [20], this work includes a gain design approach, robustness analysis to misaligned frames, and a collision avoidance strategy.

*This work was supported by the U.S. Air Force Research Laboratory under grant FA8651-17-1-0001 and the Army Research Office grant W911NF-17-1-0058.

K. Fathian, S. Safaoui, and N. R. Gans are with the Department of Electrical Engineering, T. H. Summers is with the Department of Mechanical Engineering, University of Texas at Dallas, Richardson, TX, 75080 USA. E-mail: {kaveh.fathian, sxs169833, tyler.summers, ngans }@utdallas.edu.

[1]In particular, our approach is robust to accelerometer measurement inaccuracies discussed in [19].

## II. Notation and Assumptions

We consider a team of $n \in \mathbb{N}$ agents with the inter-agent sensing topology described by an undirected graph $\mathcal{G} = (\mathcal{V}, \mathcal{E})$, where $\mathcal{V} = \mathbb{N}_n := \{1, 2, \ldots, n\}$ is the set of vertices, and $\mathcal{E} \subset \mathcal{V} \times \mathcal{V}$ is the set of edges. Each vertex of the graph represents an agent. An edge from vertex $i \in \mathcal{V}$ to $j \in \mathcal{V}$ indicates that agents $i$ and $j$ can measure the relative position of each other in their local coordinate frames. In such a case, agents $i$ and $j$ are called neighbors. The set of neighbors of agent $i$ is denoted by $\mathcal{N}_i := \{j \in \mathcal{V} \,|\, (i, j) \in \mathcal{E}\}$.

Throughout this paper, we assume that the desired formation and the sensing topology are such that achieving the formation is physically feasible. In particular, we assume that the sensing topology is undirected and universally rigid. This assumption is both necessary and sufficient [23], [24] for guaranteeing the existence of control gains that are computed from the proposed SDP approach.

## III. Formation Control for Agents with Single-Integrator Dynamics

In this section, we extend the formation control strategy introduced in [17], [18], [25] from 2D formations to 3D shapes. Our extension makes the assumption that the $z$-axes of agents' local coordinate frames are aligned[2]. However, as we will show in Section V, the control is robust to misaligned frames. The results of this section are for agents with the single-integrator dynamics (i.e., kinematic model). When applied to MAVs, the onboard controller of each MAV is responsible for directing the vehicle along the desired direction of motion with the desired speed. In Section V, we show that the disparities between the desired and actual motion of MAVs that may exist due to MAV dynamics or disturbances do not affect the convergence of agents to the desired formation.

Motion of agents with single-integrator dynamics can be expressed as

$$\dot{q}_i = u_i, \tag{1}$$

where $q_i := [x_i, y_i, z_i]^\top \in \mathbb{R}^3$ represents the coordinates of agent $i \in \mathbb{N}_n$ in a global coordinate frame (unknown to the agent), and $u_i \in \mathbb{R}^3$ is the control law. In this paper, we address the following problem.

**Problem 1.** Design control $u_i$ such that agents with dynamics (1) autonomously achieve a desired 3D formation using only local relative position measurements.

To address Problem 1, the control $u_i$ can be specified as

$$u_i := \sum_{j \in \mathcal{N}_i} A_{ij}\,(q_j - q_i), \tag{2}$$

where $q_j - q_i$ represents the relative position of agent $j$ with respect to agent $i$, and $A_{ij} \in \mathbb{R}^{3\times 3}$ are constant control gain matrices that are designed and provided to each agent before the mission and have the form

$$A_{ij} = \begin{bmatrix} a_{ij} & -b_{ij} & 0 \\ b_{ij} & a_{ij} & 0 \\ 0 & 0 & c_{ij} \end{bmatrix}. \tag{3}$$

[2]With minor changes in the design $x$ or $y$-axis can be used alternatively. Note that the first two diagonal elements of $A_{ij}$ are identical, and the off-diagonal terms only differ in sign. If the $z$-axes of agents' local coordinate frames and the global coordinate frame are aligned, from the commutativity property of $A_{ij}$ matrices (which holds due to their special structure) it follows that the closed-loop dynamics is invariant to expressing the coordinates in the global or local frames[3]. Note that the local coordinate frames do not need to be aligned along their $x$-$y$ directions. The geometric interpretation of the control (2) is explained in the following example.

**Example 1.** Consider three agents and assume that agents 2 and 3 are neighbors of agent 1. Denote by $q_2 = [2, 3, 1]^\top$ and $q_3 = [2, 1, 2]^\top$ the positions of the neighbors in agent 1's local coordinate frame, which itself is located at $q_1 = [0, 0, 0]^\top$. Assume that control gain matrices

$$A_{12} = \begin{bmatrix} 2 & -1 & 0 \\ 1 & 2 & 0 \\ 0 & 0 & -1 \end{bmatrix}, \qquad A_{13} = \begin{bmatrix} -1 & 3 & 0 \\ -3 & -1 & 0 \\ 0 & 0 & 2 \end{bmatrix}, \tag{4}$$

are provided to agent 1 before the mission. From (2), the control vector for agent 1 at the current instance of time is computed as

$$u_1 = A_{12}\,(q_2 - q_1) + A_{13}\,(q_3 - q_1) = [2, 1, 3]^\top. \tag{5}$$

From the single-integrator dynamics (1) it follows that agent 1 moves along the vector $u_1$ with a speed equal to the its magnitude. Matrices $A_{12}$ and $A_{13}$ can be interpreted geometrically as a rotation of the neighbors' relative coordinates about the $z$-axis, followed by a scaling along the $z$-direction and a scaling along the $x$-$y$ directions. One can see that these actions are independent of the local coordinate frame's position and orientation in the global frame (if $z$-axes are aligned). Hence, $q_1, q_2$ and $q_3$ can be represented in either global or local coordinate frames.

Since the closed-loop dynamics is invariant to local or global representation of coordinates, to simplify the analysis from now on we assume that $q_i$'s are expressed in the global coordinate frame. By substituting (2) in (1), the closed-loop dynamics of the agents can be collectively expressed as

$$\dot{q} = A\,q, \tag{6}$$

where $q := [q_1^\top, q_2^\top, \ldots, q_n^\top]^\top \in \mathbb{R}^{3n}$ denotes the aggregate position vector, and $A \in \mathbb{R}^{3n\times 3n}$ is the aggregate gain matrix given by

$$A = \begin{bmatrix} -\sum_{j\neq 1} A_{1j} & A_{12} & \cdots & A_{1n} \\ A_{21} & -\sum_{j\neq 2} A_{2j} & \cdots & A_{2n} \\ \vdots & & \ddots & \vdots \\ A_{n1} & A_{n2} & \cdots & -\sum_{j\neq n} A_{nj} \end{bmatrix}, \tag{7}$$

in which for $j \notin \mathcal{N}_i$ (i.e., when agents are not neighbors) the $A_{ij}$ blocks are defined as zeros. Note that the $3\times 3$ diagonal blocks of $A$ are the negative sum of the rest of the blocks

[3]When frames are aligned along their $z$-axes, replacing global coordinates $q_i^{\text{global}}$ with local coordinates $q_i^{\text{local}} = R\,q_i^{\text{global}} + T$ in (1) and (2) with $R, T$ representing the relative rotation and translation between the local and global frames does not affect the dynamics since $R, T$ are canceled.

on the same row. Hence, $A$ has a block Laplacian structure, from which it follows that vectors

$$\begin{aligned}\mathbf{1}_x &:= [1,0,0,1,0,0,\ldots,1,0,0]^\top \in \mathbb{R}^{3n}\\ \mathbf{1}_y &:= [0,1,0,0,1,0,\ldots,0,1,0]^\top \in \mathbb{R}^{3n}\\ \mathbf{1}_z &:= [0,0,1,0,0,1,\ldots,0,0,1]^\top \in \mathbb{R}^{3n}\end{aligned} \tag{8}$$

are in its kernel[4].

Consider an embedding of the desired formation shape at an arbitrary location and rotation about the $z$-axis in the global coordinate frame. Let $q_i^* \in \mathbb{R}^3$ denote the coordinates of agent $i$ at this embedding, and further denote by $\bar{q}_i^* \in \mathbb{R}^3$ coordinates rotated 90 degrees about the $z$-axis and $\bar{\bar{q}}_i^* \in \mathbb{R}^3$ coordinates projected on the $x$-$y$ plane[5]. Let

$$\begin{aligned}q^* &:= [q_1^{*\top}, q_2^{*\top}, \ldots, q_n^{*\top}]^\top \in \mathbb{R}^{3n}\\ \bar{q}^* &:= [\bar{q}_1^{*\top}, \bar{q}_2^{*\top}, \ldots, \bar{q}_n^{*\top}]^\top \in \mathbb{R}^{3n}\\ \bar{\bar{q}}^* &:= [\bar{\bar{q}}_1^{*\top}, \bar{\bar{q}}_2^{*\top}, \ldots, \bar{\bar{q}}_n^{*\top}]^\top \in \mathbb{R}^{3n}\end{aligned} \tag{9}$$

denote the corresponding aggregate coordinate vectors for all agents. The following theorem states the conditions that the gain matrices must satisfy to ensure that the desired formation emerges from the interaction of all agents.

**Theorem 1.** *Consider agents with dynamics* (1) *and control* (2). *Assume $A_{ij}$ are chosen such that in* (7)

*(i) vectors $\mathbf{1}_x, \mathbf{1}_y, \mathbf{1}_z, q^*, \bar{q}^*, \bar{\bar{q}}^*$ form a basis for* $\ker(A)$,
*(ii) all nonzero eigenvalues of $A$ have negative real parts.*

*Then agents globally converge to the desired formation up to a translation, a rotation about the z-axis, a scaling along the z-direction, and a scaling along the x-y directions of the global coordinate frame.*

We omit the proof of Theorem 1 due to page limits. The proof is straightforward, since (6) is a linear system and stable nonzero eigenvalues imply that all trajectories converge to $\ker(A)$. The kernel consists of linear combination of bases vectors, which are the formations up to the degrees of freedom stated in the theorem. To give a geometric intuition, consider a desired cube formation with 8 agents and side lengths of 2 units as shown in Fig. 2. The steady-state formations achieved under control (2) for two randomly generated initial conditions are shown in the figure. In Section VII, we augment the control by a nonlinear term to fix the scale factors along the $z$ and $x$-$y$ directions and achieve the desired formation up to a rotation and a translation.

**Remark 1.** *Kernel vectors* (8) *correspond to coinciding agents, which can be interpreted as the desired formation with the zero scale. Similarly, $\bar{\bar{q}}^*$ corresponds to formations with zero scale along the z-direction. It can be shown that the set of initial conditions from which agents converge to these kernel vectors is measure zero. In practice, trajectories cannot remain on a measure zero set (due to noise, disturbances, etc.). Furthermore, in subsequent sections we present a collision avoidance strategy and augment the control to fix the scale to a desired value. Therefore, these cases are not of practical concern.*

[4]The kernel or null space of $A \in \mathbb{R}^{n\times n}$ is $\ker(A) := \{v \in \mathbb{R}^n \,|\, Av = 0\}$.

[5]That is, if $q_i^* = [x_i, y_i, z_i]^\top$, then $\bar{q}_i^* := [-y_i, x_i, z_i]^\top$ and $\bar{\bar{q}}_i^* := [x_i, y_i, 0]^\top$.

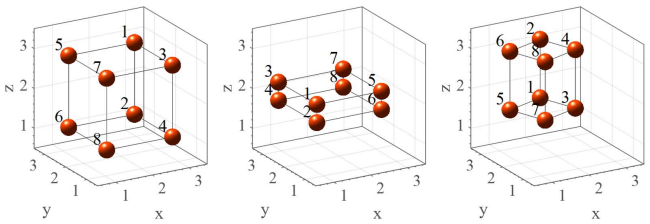


Fig. 2. (Left) A cube desired formation. (Middle and right) Formations achieved under the free-scale control (2) from two random initial conditions.

## IV. Gain Design via Optimization

Given a geometrically feasible desired formation, we proceed by showing how a set of gain matrices that meet the conditions of Theorem 1 can be found. These gains are not unique in general, and several techniques can be deployed to find a set of gains that meet the conditions of the theorem (e.g., see [24]). Our proposed approach in this section is based on a semidefinite programming (SDP) formulation, which maximizes the robustness to perturbations and measurement inaccuracies that may affect the formation, and leads to other desired properties that will be discussed in the subsequent sections.

Recall the definitions given in (8) and (9), and let $N := [q^*, \bar{q}^*, \bar{\bar{q}}^*, \mathbf{1}_x, \mathbf{1}_y, \mathbf{1}_z] \in \mathbb{R}^{3n\times 6}$ denote the desired set of bases for $\ker(A)$. Let $USV^\top = N$ be the (full) singular value decomposition (SVD) of $N$, and further let $Q \in \mathbb{R}^{3n\times(3n-6)}$ be the last $3n-6$ columns of $U$. Other than the zero eigenvalues associated to the columns of $N$, matrices $A$ and

$$\bar{A} := Q^\top A Q \ \in \mathbb{R}^{(3n-6)\times(3n-6)} \tag{10}$$

have the same set of eigenvalues. Consequently, matrix $A$ can be computed by solving the convex optimization problem

$$\begin{aligned} A \ = \ \underset{a_{ij},b_{ij},c_{ij}}{\text{argmin}} \quad & \lambda_{\max}(\bar{A}) \\ \text{subject to} \quad & AN = 0 \end{aligned} \tag{11}$$

where $\lambda_{\max}(\cdot)$ denotes the largest eigenvalue of a matrix[6]. In (11), by minimizing the largest eigenvalues of $\bar{A}$ we aim to make $\bar{A}$ as negative definite as possible, hence increasing the robustness to perturbations. Note that (11) can be formulated equivalently as a SDP problem [26] and solved using existing solvers[7].

For condition (*ii*) in Theorem 1 to be satisfied, it must hold that $\lambda_{\max}(\bar{A}) < 0$. It is therefore important to address under what conditions solving (11) results in a negative objective function. To answer this question we first note that if a set of gains for which $\lambda_{\max}(\bar{A}) < 0$ exists, it is guaranteed to be found by (11) since the problem is convex. Hence, the focus is on conditions that ensure the existence of such gains. This point is answered in the following remark.

[6]Since by assumption $A$ is symmetric, $\bar{A}$ is symmetric and its eigenvalues are real and can be ordered.

[7]We used SDPT3 solver in the CVX package [27] to solve (11).

**Algorithm 1:** Control gain design.

**input :** Desired formation coordinates $q^* \in \mathbb{R}^{3n}$.
**output:** Gain matrix $A \in \mathbb{R}^{3n\times 3n}$.

**step 1:** Let $N := [q^*, \bar{q}^*, \bar{\bar{q}}^*, \mathbf{1}_x, \mathbf{1}_y, \mathbf{1}_z]$.
**step 2:** Compute SVD of $N = USV^\top$.
**step 3:** Define $Q$ as the last $3n-6$ columns of $U$.
**step 4:** Solve (11) using a SDP solver.

**Remark 2.** *For a general desired formation shape, the necessary and sufficient conditions that guarantee the existence of A satisfying the conditions of Theorem 1 are that the sensing graph is undirected and universally rigid. These conditions have been derived in [21, Thm. 3.2], and we assume they hold throughout this paper.*

We point out that solving (11) relies on a centralized paradigm and knowledge of the sensing graph among agents. Under the assumption that agents can communicate, distributed optimization techniques can be used to solve (11) locally on each agent. An example of such distributed design can be found in [21].

## V. Robustness Properties

We proceed by showing the properties that follow from our proposed approach. The following theorem provides the main result from which several corollaries will follow.

**Theorem 2.** *Consider a symmetric gain matrix A satisfying the conditions of Theorem 1. Let $R_i \in \mathrm{SO}(3)$ denote a rotation matrix of $\theta_i$ radians about an arbitrary axis of rotation, and $c_i \in \mathbb{R}$ be a scalar. If $c_i \geq \varepsilon$ and $\theta_i \in [-\frac{\pi}{2}+\varepsilon,\ \frac{\pi}{2}-\varepsilon]$ for an arbitrary small $\varepsilon > 0$, then under the perturbed control*

$$u_i := c_i R_i \sum_{j\in\mathcal{N}_i} A_{ij}(q_j - q_i) \tag{12}$$

*agents globally converge to the desired formation (up to the degrees of freedom mentioned in Theorem 1).*

Proof of Theorem 2 is presented in the Appendix. The theorem implies that convergence of agents to the desired formation is unaffected by any positive scaling of the control vector $u_i$ defined in (2), or any rotation of this vector up to 90 degrees. In other words, the plane with normal $u_i$ divides the space into two regions, and agents are free to move along any direction in the open half space containing $u_i$.

**Remark 3.** *The results in Theorem 2 hold for any continuous or discontinuous change in $c_i$ or $R_i$ as long as the conditions of the theorem are met. This is because V in the proof can be considered as a common Lyapunov function for a family of switching systems (see [28, Chap. 2] for more details).*

**Corollary 1.** *From Theorem 2, it follows that the control* (2) *is robust to*

*(i) input saturations,*
*(ii) perturbations and noise in measurements,*
*(iii) misalignment of local coordinate frames' z-axes.*

Due to space constraints, rather than giving the formal proof, we briefly discuss the reasoning behind the statements of Corollary 1. Property (*i*) follows by observing that input saturation can be modeled as a positive downscaling of the input when its value is greater than a saturation threshold. Properties (*ii*) and (*iii*) follow by noting that the effect of measurement inaccuracies and misaligned coordinate frames can be modeled as an unwanted rotation and scaling in the desired direction of motion. Hence, from Theorem 2 convergence to the desired formation is not affected. Property (*iii*) in Corollary 1 in particular indicates that the control is robust to inaccuracies that can be caused by noise or acceleration effects in the direction of gravitational force measured by an IMU sensor used to align the local coordinate frames when the control is implemented on MAVs.

## VI. Distributed Collision Avoidance

Consider Fig. 3 illustrating the scenario discussed in Example 1, with two safety regions defined as spheres of radius one centered at agents 2 and 3. Moving along the desired control direction shown in the figure drives agent 1 into the safety sphere of agent 2, which can be undesirable and lead to a collision. To prevent entering the safety regions, from the discussion in the last section we observe that agent 1 can move along any alternative direction in the upper open half space defined by plane with normal $u_1$. This is the main idea for the distributed collision avoidance strategy outlined in Algorithm 2. In this algorithm, the control vector is rotated to a new direction that does not intersect the safety regions of adjacent agents closer than a threshold distance $d \in \mathbb{R}$. The safety regions are defined as spheres with radius $r \in \mathbb{R}$ centered at agents, however, they can take other shapes. For example, a cylindrical safety region can be considered for MAVs to avoid both collisions and air flow disturbances. It may occur that no direction in the allowed open half space exists that does not intersect with a safety region. In this case, the control is set to zero, and the agent stops until a feasible control direction becomes available.

Alternatively, one can look at Algorithm 2 as a switching control strategy, where given the desired control action $u_i$, the new control direction $u_i'$ is defined as

$$u_i' = \begin{cases} u_i & \text{if no collision} \\ Ru_i & \text{if collision possible, escape direction exists} \\ 0 & \text{if collision possible, no escape direction} \end{cases} \tag{13}$$

**Corollary 2.** *Under the collision avoidance scheme in Algorithm 2, the desired formation remains a globally stable equilibrium.*

Proof of Corollary 2 follows by noting that under Algorithm 2, any nonzero modified control direction satisfies the conditions of Theorem 2, and the stability is not affected when the control is set to zero. Unfortunately, convergence to the desired formation is not always guaranteed, and one can construct counterexamples where agents are caught in a gridlock due to unavailability of a feasible direction of motion. These gridlocks exist due to the distributed nature of the strategy. Other distributed schemes that do not use

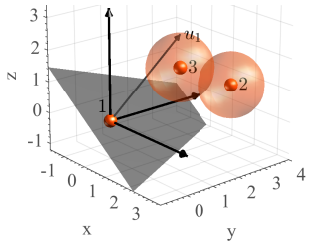


Fig. 3. Control direction $u_1$ intersects safety region of agent 3. To avoid collision, agent 1 can move along any direction in the open half space above the plane with normal $u_1$ shown in gray passing through agent 1.

**Algorithm 2:** Distributed collision avoidance.

**input :** Desired control direction $u_i \in \mathbb{R}^3$
Collision sphere radius $r \in \mathbb{R}$
Activation threshold $d \in \mathbb{R}$, $d \geq r$
**output:** Modified control direction $u_i \in \mathbb{R}^3$

**step 1:** Construct safety spheres of radius $r$ centered at agents closer than $d$.
**step 2:** Find rotation $R(\theta) \in \mathrm{SO}(3)$ with minimum $|\theta|$ and $Ru_i$ not intersecting safety spheres.
**step 3:** If step 2 is infeasible or $|\theta| \geq \frac{\pi}{2}$ set $u_i \leftarrow 0$, otherwise set $u_i \leftarrow R(\theta)u_i$.

inter-agent communication, such as safety barrier functions [29] and traffic circles [30], have similar gridlock situations. Resolving gridlocks using inter-agent communication is possible and will be discussed in our future work.

We point out that the threshold $d \geq r$ in Algorithm 2 defines a collision avoidance topology, which should not be confused with the sensing topology discussed in previous sections. For example, two nearby agents may actively modify the direction of their control vectors to avoid a collision while their relative positions are not used in computing the control direction (2). The threshold $d$ can be used to alter the control direction as little as possible by activating the collision avoidance strategy only when two agents are sufficiently close.

**Proposition 1.** *Let $d_{ij} \in \mathbb{R}$ denote the distance between agents $i$, $j$, and assume that $d_{ij} \geq r$ for all $i, j \in \mathbb{N}_n$ at time $t = t_0$. Under the collision avoidance scheme in Algorithm 2, $d_{ij} \geq r$ for all $t > t_0$.*

We omit the proof of Proposition 1 due to the page limits and only emphasize that this result is based on agents with the kinematic model (1) with control (2). For agents with higher order dynamics velocity obstacle approach [31] can be considered, and will be a topic of our future work.

## VII. Fixed-Scale Control

As discussed in Theorem 1 and illustrated in Fig. 2, under the control (2), the desired formation is achieved up to scale factors along the $z$-direction and $x$-$y$ directions. To fix the scale of the formation along all directions, (2) can be augmented by a bounded smooth map $f : \mathbb{R} \to \mathbb{R}$ as

$$u_i = \sum_{j \in \mathcal{N}_i} A_{ij}(q_j - q_i) + f(d_{ij} - d_{ij}^*)(q_j - q_i), \qquad (14)$$

where $d_{ij} := \|q_j - q_i\|$ denotes the distance between agent $i$ and $j$, $d_{ij}^* \in \mathbb{R}$ is its desired value, and $f$ is chosen such that $xf(x) > 0$ for $x \neq 0$, and $f(0) = 0$. Possible choices for $f$ are $f : x \mapsto \frac{1}{k}\arctan(x)$ or $f : x \mapsto \frac{1}{k}\tanh(x)$, where $k > 0$ is an arbitrary constant. The role of $f$ in (14) is to pull agents toward their neighbors when the distance between them is larger than the desired value, and vice versa.

**Proposition 2.** *Consider agents with dynamics* (1) *and assume $A_{ij}$ matrices satisfy the conditions of Theorem 1. Under the control* (14)*, the desired formation is a locally asymptotically stable equilibrium (up to a rotation about the z-axis and a translation in the global coordinate frame).*

Proof of Proposition 2 follows by linearizing (14) about the equilibrium $q^*$ and showing that the Jacobian matrix is negative semidefinite. The study of *global* asymptotic stability of the desired formation will be a topic of future work.

## VIII. Experimental Results

To validate the proposed strategy, Crazyflie quadrotors (Fig. 1) operated using the Crazyswarm package [32] are used in multiple experiments to show that agents can achieve a desired 3D formation without collision. The position and orientation of each quadrotor are obtained by a Vicon motion capture system. This localization scheme is centralized, so to replicate a distributed setting where the positions are relative and local, Vicon measurements are transformed into the body frame of each quadrotor before being used to compute the control direction for each vehicle. Note that the $z$-axes of body frames are not aligned in general due to the roll and pitch angles of quadrotors needed to induce motion. This effectively demonstrates the robustness of our method to misalignments in the $z$-axes that may be present in a fully-distributed implementation.

Fig. 4 shows snapshots of an experiment with 8 quadrotors at different instances of time, with the quadrotors highlighted using yellow circles. The quadrotors initially hover to an altitude of 0.5m. Control strategy (14) with collision avoidance in Algorithm 2 is used to compute a desired direction of motion for each vehicle. The low-level controller of each quadrotor is responsible for moving the vehicle along the desired direction with the yaw angle set to zero[8]. Nonzero eigenvalues of matrix $A$ computed from Algorithm 1 range from $-10$ to $-5$, and $f$ is chosen as $2.5\arctan(\cdot)$ in (14). The time required to compute $A$ on an Intel Core i7 CPU @1.73GHz and 12 GB Ram notebook is around 0.70s. The values of parameters in Algorithm 2 are chosen as $r = 0.45$m and $d = 0.5$m. The trajectory of quadrotors is shown in the rightmost figure, where the sensing graph is illustrated via lines connecting the agents and is fixed throughout the experiment. The spheres denote the position of the quadrotors at their final configuration, which coincide with the desired formation (up to a rotation about $z$-axis and a translation).

[8]The yaw angles can take other values if desired.

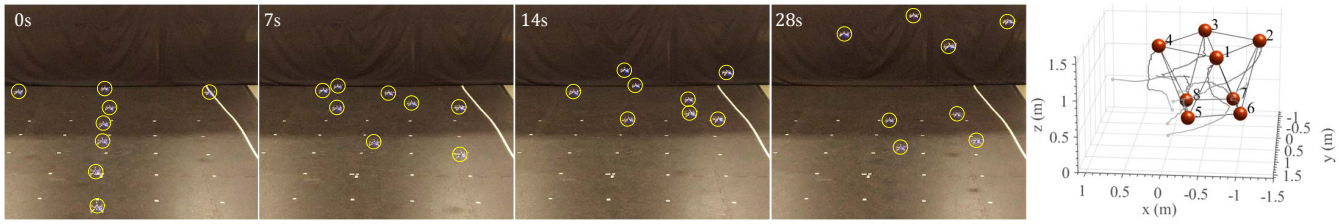


Fig. 4. Snapshots of 8 quadrotors converging to a desired formation. (Right) Trajectories and final positions reconstructed using Vicon data.

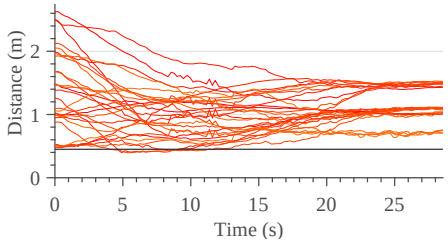


Fig. 5. All 28 inter-agent distances plotted vs. time. The safety radius $r = 0.45$m is shown via gray line.

All inter-agent distances during the experiment are plotted in Fig.5. As can be seen, the quadrotors respect the minimum safety distance of $r = 0.45$m as they converge to the desired formation[9]. A link to additional experiments and associated videos is provided in the Supplementary Material section.

## IX. Concluding Remarks and Future Work

We presented a distributed control strategy to achieve a desired 3D formation of distinct agents using only local relative position measurements. No global positioning system or centralized motion planning scheme is required, and our approach can be implemented on existing MAV platforms. We assumed that the $z$-axes of the agents' local coordinate frames are aligned, however, we showed that this assumption is not crucial and the control is robust to misaligned frames and errors in the desired direction of motion that can occur due to noise, disturbances, or unmodeled dynamics. We further presented a fully-distributed collision avoidance strategy to ensure that agents maintain a safe distance with respect to each other.

Although the analysis of this paper was centered at single-integrator agents, it is straightforward to extend the approach proposed here to agents with higher order dynamics (see our previous work [17, Sec. IV] for 2D formations). Furthermore, the sensing topology among agents can be time-varying (see our previous work [33]).

Due to the distributed nature of our collision avoidance strategy, gridlocks can occur. Incorporating a communication scheme to resolve gridlocks will be a topic of future work. Extending the collision avoidance scheme to agents with higher order dynamics using the velocity obstacle approach will also be considered. Additional research directions include leveraging leader-follower strategies for cooperative navigation of multiple MAVs, hence, allowing a single human operator to navigate a team of MAVs while they autonomously attain the desired formation.

[9]Slight violation of safety radius at time interval 5s-8s is due to the unmodeled quadrotor dynamics and does not contradict Proposition 1, which is based on a kinematic model.

## Appendix

We first present and prove the following lemma that is used in the proof of Theorem 2.

**Lemma 1.** *Let $R \in \mathrm{SO}(3)$ represent a rotation of $\theta \in [-\pi, \pi)$ radians about the unit norm rotation axis $[x, y, z]^\top \in \mathbb{R}^3$. If $|\theta| < \frac{\pi}{2}$, then $R + R^\top$ is positive definite.*

*Proof.* Matrix $R \in \mathrm{SO}(3)$ can be represented as

$$R = \begin{bmatrix} c+x^2\alpha & xy\alpha - zs & xz\alpha + ys \\ yx\alpha + zs & c+y^2\alpha & yz\alpha - xs \\ zx\alpha - ys & zy\alpha + xs & c+z^2\alpha \end{bmatrix}, \tag{15}$$

where $\alpha := 1 - c$, and $c, s$ are shorthand notations for $\cos(\theta)$, $\sin(\theta)$, respectively. Hence,

$$R + R^\top = 2\alpha \begin{bmatrix} \beta+x^2 & xy & xz \\ yx & \beta+y^2 & yz \\ zx & zy & \beta+z^2 \end{bmatrix}, \tag{16}$$

where $\beta := \frac{c}{1-c}$. Noting that $x^2 + y^2 + z^2 = 1$, eigenvalues of $R + R^\top$ are found by direct computation as $\{2\alpha,\ 2\alpha,\ 2\alpha\beta\}$, which since for $|\theta| < \frac{\pi}{2}$ we have $\alpha, \beta > 0$ matrix $R + R^\top$ is positive definite. □

We now present the proof of Theorem 2.

*Proof.* Under the perturbed control (12), the aggregate dynamics can be represented by

$$\dot{q} := PAq \tag{17}$$

where $P := \mathrm{diag}(c_1 R_1, c_2 R_2, \ldots, c_n R_n) \in \mathbb{R}^{3n \times 3n}$ is a block diagonal matrix that contains the perturbation terms.

Consider the differentiable functional $V := -q^\top A q$. Note that $V$ is positive semidefinite since by design $A$ is negative semidefinite, and $V = 0$ if and only if $q \in \ker(A)$. Noting that $A^\top = A$, derivative of $V$ along the trajectories of (17) is

$$\dot{V} = -\dot{q}^\top A q - q^\top A \dot{q} = -q^\top A \left(P^\top + P\right) A q. \tag{18}$$

Matrix $P^\top + P$ is block diagonal and each diagonal block is given by $c_i (R_i^\top + R_i) \in \mathbb{R}^{3\times 3}$. From Lemma 1 we have that if $|\theta_i| < \frac{\pi}{2}$ and $c_i > 0$ for all $i \in \{1, \ldots, n\}$, then all diagonal blocks are positive definite. This implies that $P^\top + P$ is positive definite, and consequently $\dot{V} < 0$ for all $q \notin \ker(A)$. From the Lyapunov stability theory and LaSalle's invariance principle [34] it then follows that all trajectories of (17) converge to the invariant set $q \in \ker(A)$. □

## REFERENCES


[1] T. Cieslewski, S. Choudhary, and D. Scaramuzza, "Data-efficient decentralized visual SLAM," in *IEEE International Conference on Robotics and Automation*, 2018.

[2] T. Ozaslan, G. Loianno, J. Keller, C. Taylor, V. Kumar, J. Wozencraft, and T. Hood, "Autonomous navigation and mapping for inspection of penstocks and tunnels with MAVs," *IEEE Robotics and Automation Letters*, vol. 2, no. 3, pp. 1740–1747, 2017.

[3] K. Dorling, J. Heinrichs, G. G. Messier, and S. Magierowski, "Vehicle routing problems for drone delivery," *IEEE Transactions on Systems, Man, and Cybernetics: Systems*, vol. 47, no. 1, pp. 70–85, 2017.

[4] R. Bahnemann, D. Schindler, M. Kamel, R. Siegwart, and J. Nieto, "A decentralized multi-agent unmanned aerial system to search, pick up, and relocate objects," in *IEEE International Symposium on Safety, Security and Rescue Robotics*, Oct 2017, pp. 123–128.

[5] J. C. Barca and Y. A. Sekercioglu, "Swarm robotics reviewed," *Robotica*, vol. 31, no. 3, pp. 345–359, 2013.

[6] Z. Yan, N. Jouandeau, and A. A. Cherif, "A survey and analysis of multi-robot coordination," *International Journal of Advanced Robotic Systems*, vol. 10, no. 12, p. 399, 2013.

[7] K.-K. Oh, M.-C. Park, and H.-S. Ahn, "A survey of multi-agent formation control," *Automatica*, vol. 53, pp. 424–440, 2015.

[8] N. Michael, M. M. Zavlanos, V. Kumar, and G. J. Pappas, "Distributed multi-robot task assignment and formation control," in *IEEE International Conference on Robotics and Automation*, 2008, pp. 128–133.

[9] M. Aranda, G. López-Nicolás, C. Sagüés, and M. M. Zavlanos, "Coordinate-free formation stabilization based on relative position measurements," *Automatica*, vol. 57, pp. 11–20, 2015.

[10] N.-s. P. Hyun, P. A. Vela, and E. I. Verriest, "Collision free and permutation invariant formation control using the root locus principle," in *American Control Conference*, 2016, pp. 2572–2577.

[11] T. Motoyama and K. Cai, "Top-down synthesis of multi-agent formation control: An eigenstructure assignment based approach," in *American Control Conference*. IEEE, 2017, pp. 259–264.

[12] M. H. Trinh, S. Zhao, Z. Sun, D. Zelazo, B. D. Anderson, and H.-S. Ahn, "Bearing-based formation control of a group of agents with leader-first follower structure," *IEEE Transactions on Automatic Control*, 2018.

[13] K. Fathian, D. I. Rachinskii, M. W. Spong, and N. R. Gans, "Globally asymptotically stable distributed control for distance and bearing based multi-agent formations," in *American Control Conference*, 2016, pp. 4642–4648.

[14] K. Fathian, D. I. Rachinskii, T. H. Summers, and N. R. Gans, "Distributed control of cyclic formations with local relative position measurements," in *IEEE Conference on Decision and Control*, 2016, pp. 49–56.

[15] T. Han, Z. Lin, R. Zheng, and M. Fu, "A barycentric coordinate-based approach to formation control under directed and switching sensing graphs," *IEEE Transactions on cybernetics*, vol. 48, no. 4, pp. 1202–1215, 2018.

[16] K. Fathian, E. Doucette, J. W. Curtis, and N. R. Gans, "Vision-based distributed formation control of unmanned aerial vehicles," *arXiv preprint arXiv:1809.00096*, 2018.

[17] K. Fathian, T. H. Summers, and N. R. Gans, "Robust distributed formation control of agents with higher-order dynamics," *Control Systems Letters*, 2018.

[18] K. Fathian, S. Safaoui, T. H. Summers, and N. R. Gans, "Robust distributed planar formation control for higher-order holonomic and nonholonomic agents," *arXiv preprint, arXiv:1807.11058*, 2018.

[19] R. C. Leishman, J. Macdonald, R. W. Beard, and T. W. McLain, "Quadrotors and accelerometers: State estimation with an improved dynamic model," *IEEE Control Systems Magazine*, 2014.

[20] T. Han, Z. Lin, Y. Xu, R. Zheng, and H. Zhang, "Formation control of heterogeneous agents over directed graphs," in *Conference on Decision and Control*. IEEE, 2016, pp. 3493–3498.

[21] Z. Lin, L. Wang, Z. Chen, M. Fu, and Z. Han, "Necessary and sufficient graphical conditions for affine formation control," *IEEE Transactions on Automatic Control*, vol. 61, no. 10, pp. 2877–2891, 2016.

[22] S. Zhao, D. V. Dimarogonas, Z. Sun, and D. Bauso, "A general approach to coordination control of mobile agents with motion constraints," *IEEE Transactions on Automatic Control*, 2017.

[23] L. Wang, Z. Han, and Z. Lin, "Realizability of similar formation and local control of directed multi-agent networks in discrete-time," in *IEEE Conference on Decision and Control*, 2013, pp. 6037–6042.

[24] Z. Lin, L. Wang, Z. Han, and v. Minyue Fu, "A graph laplacian approach to coordinate-free formation stabilization for directed networks," *IEEE Transactions on Automatic Control*, vol. 61, no. 5, pp. 1269–1280, May 2016.

[25] Z. Lin, L. Wang, Z. Han, and M. Fu, "Distributed formation control of multi-agent systems using complex laplacian," *IEEE Transactions on Automatic Control*, vol. 59, no. 7, pp. 1765–1777, July 2014.

[26] S. Boyd, "Convex optimization of graph laplacian eigenvalues," in *Proceedings of the International Congress of Mathematicians*, vol. 3, no. 1-3, 2006, pp. 1311–1319.

[27] M. Grant and S. Boyd, "CVX: Matlab software for disciplined convex programming, version 2.1," http://cvxr.com/cvx, Mar. 2014.

[28] D. Liberzon, *Switching in systems and control*. Springer Science & Business Media, 2012.

[29] L. Wang, A. D. Ames, and M. Egerstedt, "Safety barrier certificates for collisions-free multirobot systems," *IEEE Transactions on Robotics*, vol. 33, no. 3, pp. 661–674, 2017.

[30] J. Jin, Y.-G. Kim, S.-G. Wee, and N. Gans, "Decentralized cooperative mean approach to collision avoidance for nonholonomic mobile robots," in *International Conference on Robotics and Automation*. IEEE, 2015, pp. 35–41.

[31] J. Van den Berg, M. Lin, and D. Manocha, "Reciprocal velocity obstacles for real-time multi-agent navigation," in *International Conference on Robotics and Automation*. IEEE, 2008, pp. 1928–1935.

[32] J. A. Preiss, W. Honig, G. S. Sukhatme, and N. Ayanian, "Crazyswarm: A large nano-quadcopter swarm," in *IEEE International Conference on Robotics and Automation*, 2017, pp. 3299–3304.

[33] K. Fathian, D. I. Rachinskii, T. H. Summers, M. W. Spong, and N. R. Gans, "Distributed formation control under arbitrarily changing topology," in *American Control Conference*, 2017, pp. 271–278.

[34] H. K. Khalil, "Noninear systems," *Prentice-Hall, New Jersey*, vol. 2, no. 5, pp. 5–1, 1996.